spectroscopy in both the visible and near-infrared. In the latter, a thermochromic transition is observed at 12 °C with the UV absorption shifting from 372 to 332 nm. Spectroscopic results indicate that poly(di-*n*-hexylgermane) side chains adopt a trans-planar conformation similar to those of PDHS studied previously. In addition, FT-Raman studies of PDHG provided evidence that the interaction between the *n*-hexyl side chains was similar to that found in PDHS, suggesting that the germanium backbone, like its silicon analogue, can adopt a planar, zigzag conformation. Recent WAXD studies on oriented-PDHG samples have confirmed these findings.

The lowering of the transition temperature to +12 °C (compared to 42 °C for PDHS) is thought to reflect the larger Ge–Ge bond distances, which allow the onset of disorder to occur at lower temperatures. At the transition, the *n*-hexyl side chains disorder due to the introduction of gauche bonds. This change in interaction between the hexyl side chains allows the Ge backbone to adopt a disordered conformation, which somewhat interrupts the electronic overlap and results in a shift in absorption from 372 to 332 nm.

References and Notes

(1) Miller, R. D.; Hofer, D.; Rabolt, J. F.; Fickes, G. N. *J. Am. Chem. Soc.* **1985**, *107*, 2172.
(2) Rabolt, J. F.; Hofer, D.; Miller, R. D.; Fickes, G. N. *Macromolecules* **1986**, *19*, 611.
(3) Schilling, F. C.; Bovey, F. A.; Lovinger, A. J.; Ziegler, J. M. *Bull. Am. Phys. Soc.* **1988**, *33*, 657.
(4) Miller, R. D.; Farmer, B. L.; Fleming, W. W.; Sooriyakumaran, R.; Rabolt, J. F. *J. Am. Chem. Soc.* **1987**, *109*, 2509.
(5) Farmer, B. L.; Miller, R. D.; Rabolt, J. F.; Fleming, W. W.; Fickes, G. N. *Bull. Am. Phys. Soc.* **1988**, *33*, 657.
(6) Kuzmany, H.; Rabolt, J. F.; Farmer, B. L.; Miller, R. D. *J. Chem. Phys.* **1986**, *85*, 7413.
(7) Hallmark, V. M.; Zimba, C. G.; Swalen, J. D.; Rabolt, J. F. *Spectroscopy* **1987**, *2*, 40.
(8) Zimba, C. G.; Hallmark, V. M.; Swalen, J. D.; Rabolt, J. F. *Appl. Spectrosc.* **1987**, *41*, 721.
(9) Miller, R. D.; Sooriyakumaran, R. *J. Polym. Sci., Polym. Chem. Ed.* **1987**, *25*, 111.
(10) Hallmark, V. M.; Sooriyakumaran, R.; Miller, R. D.; Rabolt, J. F. *J. Chem. Phys.* **1989**, *90*, 2486.
(11) Snyder, R. G.; Scherer, J. R.; Gaber, B. P. *Biochim. Biophys. Acta* **1980**, *601*, 47.
(12) Snyder, R. G.; Hsu, S. L.; Krimm, S. *Spectrochim. Acta* **1978**, *34A*, 395.
(13) Hendra, P. J.; Jobic, H. P.; Marsden, E. P.; Bloor, D. *Spectrochim. Acta* **1978**, *33A*, 445.
(14) Lippert, J. L.; Peticolas, W. L. *Biochim. Biophys. Acta* **1972**, *282*, 8.
(15) Farmer, B. L., private communication.

Registry No. PDHGe (homopolymer), 107310-68-9; PDHGe (SRU), 107258-58-2; 2,2-di-*n*-butyl-1,1,1,3,3,3-hexamethyltrigermane, 125330-39-4; chlorotrimethylgermane, 1529-47-1; dichlorodi-*n*-butylgermane, 4593-81-1; decamethyltetragermane, 14938-41-1; hexamethyldigermane, 993-52-2; chloropentamethyldigermane, 22640-93-3.

A Study of the Isothermal Crystallization Kinetics of Polyphosphazene Polymers. 2. Poly[bis(trifluoroethoxy)phosphazene]

Richard J. Ciora, Jr., and Joseph H. Magill*

Material Science and Engineering Department, University of Pittsburgh, Pittsburgh, Pennsylvania 15261. *Received June 1, 1989; Revised Manuscript Received November 7, 1989*

ABSTRACT: The kinetics of isothermal crystallization of poly[bis(trifluoroethoxy)phosphazene] have been studied utilizing (i) a modified differential scanning calorimeter (DSC) technique and (ii) a depolarized light intensity (DLI) technique. The kinetics of transformation of the isotropic to 2-D pseudohexagonal mesophase (i.e. the sub T_m transformation) as well as the mesophase to 3-D orthorhombic phase (i.e. the sub $T(1)$ transformation) have been measured and analyzed by using Avrami analysis. Classical nucleation theory has been applied for estimating the interfacial surface free energy values for nucleation/crystallization behavior corresponding to the phase transformations in the sub $T(1)$ and sub T_m regions. In each instance the crystallization kinetics exhibit a very strong sensitivity to undercooling over a limited temperature span. Associated with each first-order transformation, the interfacial surface free energies are more than an order of magnitude lower than values obtained in the crystallization of regular homopolymers because of the more mutually compatible (mesophase) interfaces.

Introduction

The most recently developed inorganic based polymers that show considerable commercial potential are the polyphosphazene polymers. In general the polyphosphazene polymers consist of a chain backbone of alternating phosphorous and nitrogen atoms as illustrated in Figure 1. Common substituents on the phosphorous atom may include aryl, alkyl, aryloxy, alkoxy, amino, and halogens as well as several metal atoms and inorganic groups. Different kinds of substituents on the phosphorous atom provide polymers that possess a wide variety of properties.[1,2]

An interesting feature of these polymers is the fact that many of them exhibit mesophase behavior when heated from the three-dimensionally ordered crystalline state to the isotropic melt. The atomic/molecular structure of these phases for several polyphosphazenes is known.[3,4] The effect of thermal cycling on the structure as well as the transition temperatures and enthalpies of these poly-

0024-9297/90/2223-2350$02.50/0

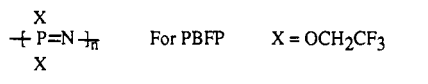

Figure 1. The basic alternating phosphorous–nitrogen structure of the poly(phosphazene) polymer.

Table I
Characterization Data of the PBFP Sample[a]

density (γ-form)[a]	1.7 g/cm^3
unit cell dimens (γ-form)	
a_0	2.06 nm
b_0	0.94 nm
c_0	0.49 nm
unit cell dimens (hexagonal form)[b] $a(200)$	1.18 nm
mesophase transition temp, $T(1)$	89.5 °C
melting transition temp, T_m	244.1 °C
glass transition temp, T_g	−66.0 °C
ΔH_f at T_m	3.77 J/g
ΔH_f at $T(1)$	51.9 J/g

[a] γ-form designates the 3-D orthorhombic structure of many of the poly(phosphazene) polymers. [b] Hexagonal form designates the general structure of the 2-D mesophase of these polymers. Thermal data for PBFP; this work.

mers in the bulk has also been investigated.[5] However the structure data can only yield information pertaining to the end states of the transformations between the phases.[6] Very little information is obtained concerning the mechanisms or energetics that control the transformation between the various phases. Through bulk isothermal crystallization rate studies, insight into the formation of the various crystalline phases may be ascertained.

Since the early 1970s the transformation kinetics of mesophase forming materials have been examined through the use of the familiar Avrami equation and classical nucleation theory. Although the literature is sparce, it does include isotropic melt to mesophase, mesophase to mesophase (if the material displays several intermediate phases), and mesophase to crystalline transformations for small molecules[7-14] and macromolecules.[15-17] In this study, part 2 of a series of papers, the kinetics of isothermal crystallization for the (a) isotropic melt to mesophase and (b) mesophase to 3-D ordered crystal transformations of the polyphosphazene polymer, poly[bis(trifluoroethoxy)phosphazene] or PBFP, are examined via (i) the depolarized light intensity (DLI) technique and (ii) a modified differential scanning calorimeter technique. The versatility of the DLI technique for investigating phase transformations in polyphosphazenes was examined in part 1.[18] In the next paper in this series (part 3), poly[bis(phenylphenoxy)phosphazene] or PB(4-Ph)PP will be considered and compared to PBFP.

The objectives of this research are essentially 3-fold: (1) to establish and quantify the rate at which PBFP crystallizes, (2) to establish the type and/or mode of crystallization by which this polymer crystallizes, and (3) to examine the nature and energetics of the crystallization process in this polymer. The data generated provides a suitable basis for the comparison of the two techniques (DSC and DLI). A secondary objective of this research examines the efficacy and utility of the two methods.

Experimental Section

Material. In this study the polyphosphazene polymer, poly[bis(trifluoroethoxy)phosphazene] (PBFP), was investigated. The sample was synthesized via the solution polymerization technique.[19] On heating it exhibits three thermal transitions, a glass transition, T_g, and two first-order transitions. The first transition at $T(1)$ corresponds to a change from a three-dimensional orthorhombic structure (the chain extended γ-form, see ref 3) to a two-dimensional pseudohexagonal structure (thermotropic δ-form) followed by a melting transition at T_m, above which an isotropic phase exists. This material was characterized by DSC, X-ray, and ^{31}P solution NMR. The NMR results revealed that PBFP did not exhibit cross-linking or branching. Characterization data relevant to PBFP is listed in Table I.

Equipment. DSC measurements were performed by using a calibrated Perkin-Elmer DSC-2 equipped with a scanning autozero and interfaced with an IBM-PC for data acquisition. High purity standards of indium, tin, lead, and zinc were used to calibrate the calorimeter. All experimental measurements were performed in a nitrogen atmosphere and a low-temperature dry ice/ethanol bath was utilized for rapid thermal equilibration during sample quenching operations. Maximum range sensitivity of 0.1 mcal/s was used for all experimental determinations. Samples between 8 and 12 mg were sealed in aluminum pans. Isothermal crystallization measurements at several temperatures were carried out by DSC in both the sub T_m and sub $T(1)$ regions for PBFP.

Depolarized light intensity, DLI, measurements were carried out by using a Hacker Instruments polarizing microscope fitted with a photodiode for measuring light intensity. The signal from the photodiode was amplified via a Phillips PM5170 amplifier and then recorded on a Hitachi Ltd. strip chart recorder. Temperature control of the stage was accomplished by using a calibrated Mettler FP-2 hotstage. Nitrogen was used to purge the stage at all times to prevent sample degradation. Samples weighed less than 1 mg and were placed between glass coverslips. Isothermal crystallization measurements at several temperatures were carried out only in the sub T_m region for PBFP.

For both the DSC and DLI techniques, the sample was first fused above its melting temperature to remove previous thermal history and then quenched to the desired crystallization temperature (40 °C/min via DSC and ~25 °C/min via DLI).

Photomicrographs were taken during phase transformations in only the sub T_m region for PBFP with a Leica 35-mm camera using Kodak Tri-X pan (ASA) 400 speed film.

Theory

To characterize the rate and mode of crystallization, the familiar Avrami equation

$$X(t) = 1 - \exp(-kt^n) \tag{1}$$

was used where k is a temperature-dependent rate constant and n describes the mode of nucleation and crystal growth and is usually an integer between 1 and 4. $X(t)$ represents the fraction of transformed or crystallized material after time, t. In the DSC technique $X(t)$ is expressed as

$$X(t) = \frac{\Delta H_t}{\Delta H_\infty} = \frac{\int_0^t E_t\,dt}{\int_0^\infty E_t\,dt} \tag{2}$$

where ΔH_t is the enthalpy change at time, t, ΔH_∞ is the total enthalpy change of the system, and E_t is the rate of energy evolution at time, t. In the depolarized light intensity[20] (DLI) technique it is expressed as

$$X(t) = \frac{I_\infty - I_t}{I_\infty - I_0} \tag{3}$$

where I_∞, I_0, and I_t represent the transmitted light intensity at long time, at initial time, and at intermediate time, t, respectively. Avrami theory is useful for determining the mode of crystal nucleation (heterogeneous or homogeneous), the crystal growth habit (spherical, circular, etc.), and the overall rate at which crystallization proceeds.

Crystallization in polymeric materials is generally nucleation-controlled. By means of classical nucleation theory the energetics of formation of the nuclei are examined. Turnbull and Fisher[21] have shown the rate at which

Table II
Functions for ΔG^* for Several Modes of Nucleation Based on a Rectangular Equilibrium Shape[a]

3-D Primary Nucleation
$\Delta G^*_{het} = 32\sigma\Delta\sigma\sigma_e/\delta f^2$
$\Delta G^*_{hom} = 32\sigma^2\epsilon_e/\delta f^2$
2-D Primary Nucleation
$\Delta G^*_{het} = 4l^2\sigma\Delta\sigma/(l\delta f - 2\sigma_e)$
$\Delta G^*_{hom} = 4l^2\sigma^2/(l\delta f - 2\sigma_e)$
Coherent Secondary Nucleation
$\Delta G^*_g = 4b_0\sigma\sigma_e/gf$ where
$\delta f = \Delta H_f\Delta T/T_m^0$

[a] Also shown is the function for ΔG_g^* for coherent, secondary nucleation.

nucleation occurs at constant temperature and pressure is given by

$$N = N_0 \exp(-\Delta E/k_b T_c) \exp(-\Delta G^*/k_b T_c) \quad (4)$$

where N is the nucleation rate, N_0 is a preexponential temperature independent constant, ΔE is the temperature-dependent energy of activation for transport from the isotropic phase, ΔG^* is the critical free energy of the critical sized nuclei, and k_b and T_c are the Boltzmann constant and the crystallization temperature, respectively.

If the linear crystal growth rate, G, is assumed to be a nucleation-controlled process, then nucleation theory may be utilized to describe the linear growth rate of the crystalline phase as

$$G = G_0 \exp(-\Delta E/k_b T_c) \exp(-\Delta G^*_g/k_b T_c) \quad (5)$$

where ΔG^*_g is the free energy of formation of the secondary nuclei. ΔG^* and ΔG_g^* have been evaluated by several authors. Table II shows various functions for ΔG^* for different modes of nucleation specifically, 3-D and 2-D heterogeneous and homogeneous primary nucleation based on a rectangular equilibrium shape. Also shown is the equation for secondary nucleation for the coherent, heterogeneous mechanism.

In the absence of independent values of N and G, the Avrami temperature-dependent rate parameter, k, may be utilized through the relationship

$$k \sim NG^z \quad (6)$$

where z is the growth dimensionality of the macroscopic crystallites (and is not equivalent to the Avrami n when the nucleation is homogeneous). From eqs 4 and 5 it is possible to generate an equation of the form

$$\ln k \sim C_0 - \Delta G^*/k_b T_c - \frac{4zb_0\sigma\sigma_e T_m^0}{k_b \Delta H T_c \Delta T} \quad (7)$$

where C_0 is a constant embodying G_0 and N_0 as well as the transport term, ΔE, whose temperature sensitivity is small compared to the free energy terms at small undercooling. Information about the surface free energies of the critical nuclei may be obtained from the slope of a plot of $\ln k$ versus $1/T_c\Delta T$ or $1/T_c\Delta T^2$.

The limitations of the Avrami and classical nucleation theories with respect to polymeric systems have been documented,[22,23] but, with these restrictions in mind, it is possible to gain insights into the mechanics and energetics of the crystallization transformations in these systems.

Results and Discussion

Transformations in PBFP. (a) Isotropic Melt to 2-D Region. The rate of energy evolution with time curves are shown in Figure 2 for the isothermal crystallization

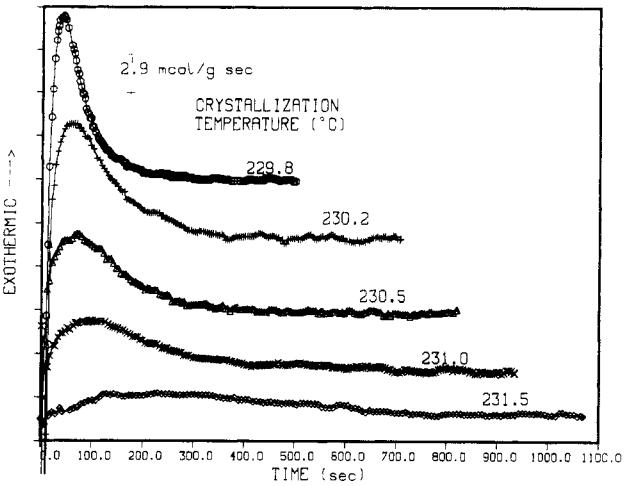

Figure 2. Rate of energy evolution versus time curves for PBFP at several crystallization temperatures for the isotropic melt to 2-D hexagonal mesophase crystallization transformation.

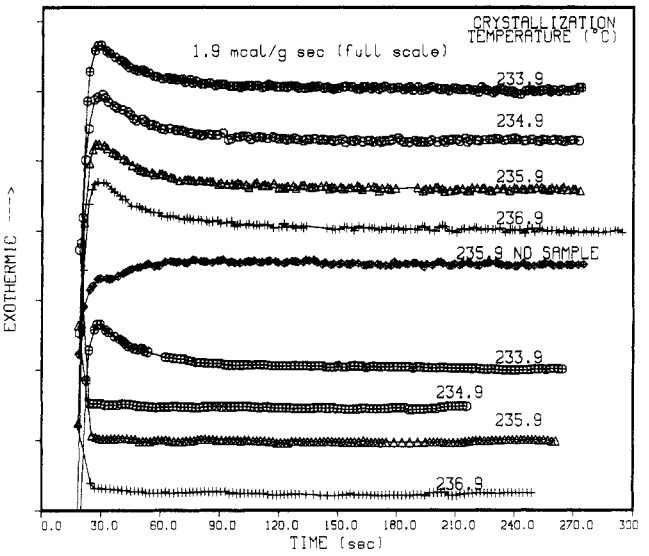

Figure 3. Isothermal curves for PBFP and an empty sample pan for the given temperatures before (top) and after (bottom) subtraction of the curve at 233.9 °C from the others.

transformation of PBFP from the isotropic melt to the two-dimensional pseudohexagonal mesophase. Significant curvature occurs in Avrami plots of these data at short times and low conversions if the rate of energy evolution, E_t, is not measured properly. This problem arises as a result of fluctuations in the energy signal from the DSC at short times (~30–120 seconds) following mode switching operations, specifically from cooling to isothermal operations or from isothermal to heating operations. An isothermal base-line subtraction technique and a short time extent of conversion recovery technique were employed to predict correctly the short time extent of conversion.

The isothermal base-line subtraction technique involves repeating a crystallization run at a temperature at which the sample does not crystallize over an extended time (several hours). This particular curve will display the error associated with the fluctuations in the energy signal at short time, independent of the energy associated with crystallization. This curve therefore must be be subtracted from the isothermal curves obtained at lower temperatures where crystallization will occur. The top four curves of Figure 3 show isothermal runs for a PBFP sample conducted at 233.9, 234.9, 235.9, and 236.9 °C, respectively, several degrees above the highest temperature at

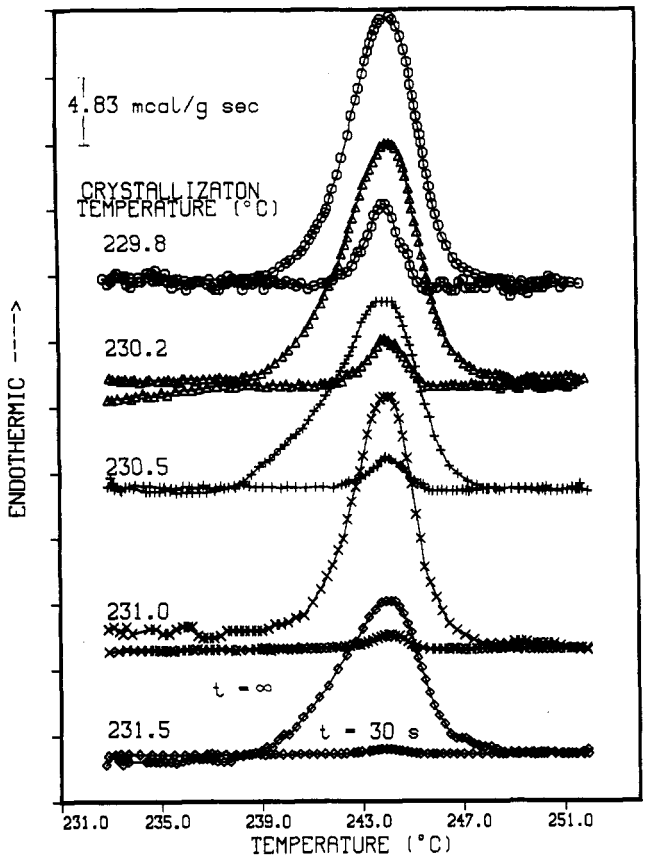

Figure 4. Fusion curves for the 2-D mesophase to isotropic melt transition in PBFP after crystallization for the times and temperatures given. Heating rate was 5 °C/min.

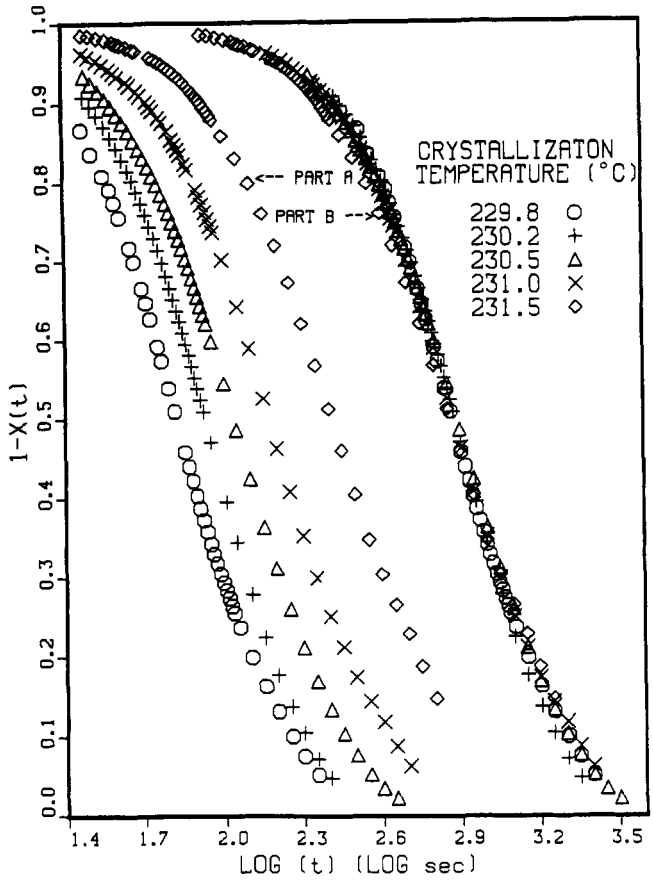

Figure 5. The extent of transformation versus log time curves for PBFP at several crystallization temperatures for the isotropic melt to 2-D mesophase transformation via the DSC method. Part A: the actual curves. Part B: these curves shifted along the log t axis (i.e. superimposed).

which PBFP is observed to crystallize over an extended time period. Nonlinearity in the isotherms (due to instrumental equilibration) persists out to roughly 120 s even though crystallization is not occurring. The bottom three curves of this figure illustrate the result of subtracting the isotherm conducted at 233.9 °C from the other curves and show that recovery of the energy signal from about 120 to roughly 30 s is possible. Also shown in Figure 3 is a "no sample" (empty pan) isothermal run conducted at 235.9 °C. It is apparent that this curve does not display the same characteristic shape as the other curves and therefore would not be suitable for use as a base line. Overall with this method a large fraction of the initial crystallization exotherm may be recovered by subtracting a high-temperature, noncrystallizing isotherm from the low-temperature, crystallizing isotherms.

A recrystallization/reheating technique is used to obtain the crucial first 30 s of data that is unrecoverable even after the isothermal base-line subtraction is performed. The procedure simply involves comparing the heats of fusion corresponding to crystallizations made for short times (in this case 30 s) to those conducted for long times. Figure 4 shows the fusion curves for samples of PBFP crystallized for 30 s and for long times. Comparing the areas under the curves at each temperature provides values for the extent of conversion at 30 s.

With these two corrections it is possible to obtain the extent of transformation with log time curves as shown in Figure 5. It is readily apparent from Figure 5, part B, that these curves are superposable, indicating that, consistent with the Avrami theory, the transformation kinetics display the same nucleation and growth mechanism.

The Avrami plots of this transformation obtained from the DSC data are shown in Figure 6. If the initial area under the rate of energy evolution curves is not predicted correctly, significant curvature in the short time, low conversion end of these plots will be introduced (this will be discussed more fully in the next section). The recovery techniques discussed above decrease significantly the curvature in these plots and thereby facilitate the measurement of the slope in this region. From linear least-squares fits of the data in the initial linear portion of each curve, an average value of n was determined to be 2.06 ± 0.11. Taking an n of 2.0, values of k, expressed as $s^{-2.0}$, were calculated at a fractional conversion of 0.25. Table III contains values of n and k obtained from these plots.

Shown in Figure 7 are the fractional conversion versus log time plots for the DLI measurements made with PBFP for the isotropic melt to 2-D pseudohexagonal mesophase transformation. From part B of this figure, good superposability of the isothermals is apparent. Avrami plots of these data are shown in Figure 8. The average value of n was determined to be 1.93 ± 0.07 (by least squares). The k parameters shown in Table IV were evaluated at a fractional conversion of 0.25 with n of 2.

Photomicrographs of this transformation in Figure 9 show the primary nucleation is independent of time (athermal, heterogeneous) at constant crystallization temperature. Considering both the DSC and DLI techniques, which provide an $n \sim 2$ for this transformation, it follows that the growth habit of the crystallites is two-dimensional from heterogeneous nuclei. Superficially, the kinetic results appear to be at variance with the photographic evidence which suggest "needlelike" crystallites

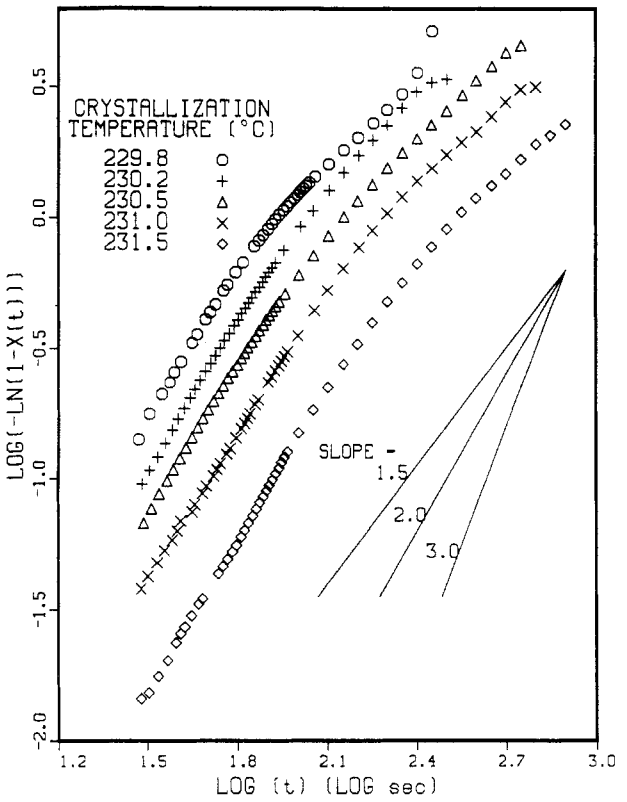

Figure 6. DSC Avrami plots for the isotropic melt to 2-D mesophase transformation in PBFP.

Table III
Values for the Avrami Parameters, n and k, for the Isotropic Melt to 2-D Mesophase Transformation in PBFP Obtained from the DSC Measurements

T_c, °C	n	10^7k, $s^{-2.0}$	ΔT, °C
229.8	2.21	1810	14.3
230.2	2.16	913	13.9
230.5	2.02	644	13.6
231.0	1.95	477	13.1
231.5	1.98	186	12.6

$n_{av} = 2.06 \pm 0.11$

and hence would correspond to an Avrami n of 1 (one-dimensional, heterogeneous growth). However closer inspection of the micrographs clearly indicates that the crystallites are platelike (see for example the micrographs shown at 420 and 5000s in parts b and c of Figure 9, respectively). The crystallites that appear "needlelike" are actually plates that have a growth direction oriented parallel or closely parallel to the polarized light beam. As this growth direction is rotated out of the position parallel to the light beam, the crystallite thickness parallel to the light beam diminishes and the resulting transmitted intensity (which is proportional to the crystallite thickness squared for thin crystals) from the platelets weakens. It is notable that the crystallites that display the weakest intensity, especially those in Figure 9c, exhibit a 2-D geometry. Thus the micrographs show randomly oriented birefringent platelets growing in two dimensions from heterogeneously activated nuclei, consistent with the kinetic results.

Plots of ln k versus $1/T_c\Delta T$ and $1/T_c\Delta T^2$ are illustrated in Figures 10 and 11 for the DSC and DLI methods, respectively. In both cases at comparable crystallization temperatures, k values obtained by the DSC and DLI methods are in agreement. *The temperature sensitivity of k is extremely large and negative, decreasing 4 orders of magnitude in a crystallization range of 6 °C.*

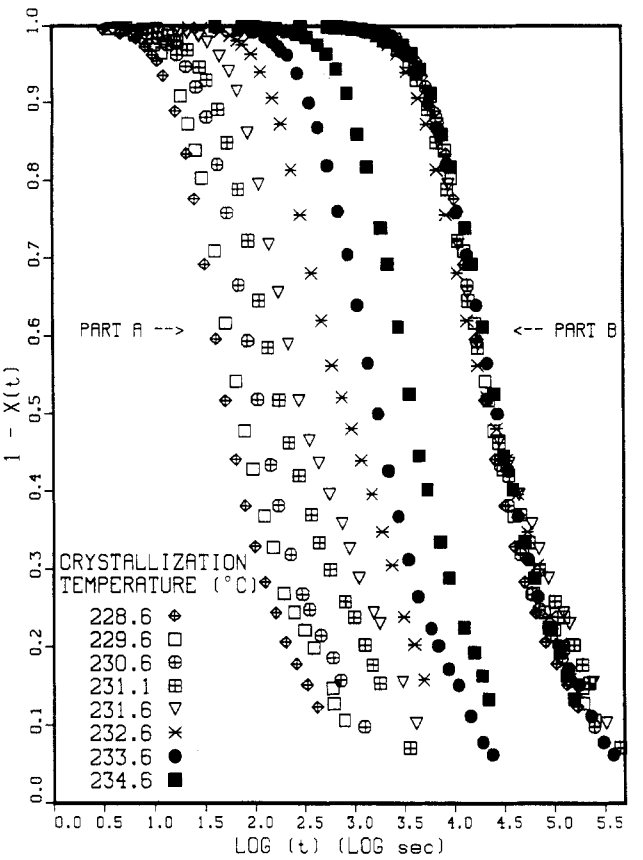

Figure 7. The extent of transformation versus log time curves for PBFP at several crystallization temperatures for the isotropic melt to 2-D mesophase transformation via the DLI method. Part A: the actual curves. Part B: these curves shifted along the log t axis (i.e. superimposed).

This large temperature dependence of k suggests nucleation control, via primary and/or secondary nucleation, for the overall transformation to the 2-D mesophase.

Only from the DLI data is it readily apparent that the plot versus $1/T_c\Delta T$ is linear. The slopes of the plots of ln k versus $1/T_c\Delta T$ obtained via the DSC and DLI techniques were −74 900 and −96 100 K^2, respectively. Assuming that the model for 2-D heterogeneous primary nucleation is applicable for the calculation of the surface energies of the critical nuclei, then $\Delta G^* = 4l^2\sigma\Delta\sigma/(l\delta f - 2\sigma_e)$ may be applied to eq 7, yielding an equation of the form

$$\ln k \sim C_0 - \left\{\frac{4l^2\sigma\Delta\sigma}{\left(\frac{l\Delta H\Delta T}{T_m^0} - 2\sigma_e\right)} + \frac{4zb_0\sigma\sigma_e T_m^0}{\Delta H\Delta T}\right\}\left\{\frac{1}{k_b T_c}\right\} \quad (8)$$

Two conditions apply to explain the linearity of the plots of ln k versus $1/T_c\Delta T$, specifically (i) when $2\sigma_e \ll l\delta f$ or (ii) when $\sigma\Delta\sigma \ll \sigma\sigma_e$. The first condition is inappropriate, since it can be shown that for $2\sigma_e \sim 0.1\ l\delta f$, σ would be less than $\Delta\sigma$ and homogeneous primary nucleation would be favored over heterogeneous nucleation. This is not borne out in the photomicrographs nor in most crystallization studies of normal homopolymers at such small undercoolings. The second condition results when primary nucleation occurs in cracks, folds, ledges, etc., as opposed to a flat substrate. This would reduce the surface energy product, $\sigma\Delta\sigma$, in the second term; thus ln k would be dominated by the third term (the linear growth term). The photomicrographs of the transformation show that the linear growth rate appears more sensitive to temperature than the primary nucleation density over this

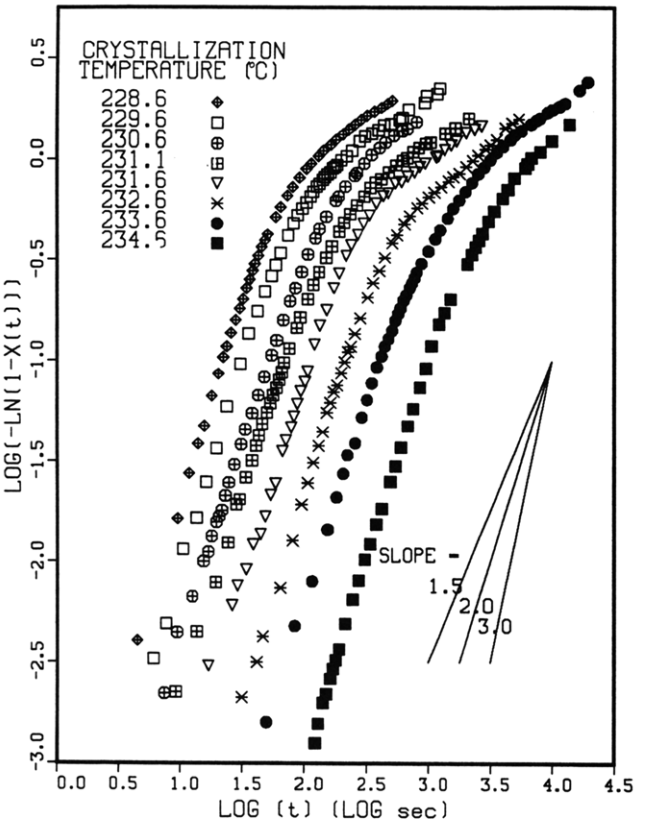

Figure 8. DLI Avrami plots for the isotropic melt to 2-D mesophase transformation in PBFP.

Table IV
Values for the Avrami Parameters, n and k, for the Isotropic Melt to 2-D Mesophase Transformation in PBFP Obtained from the DLI Measurements

T_c °C	n	10^7k, $s^{-2.0}$	ΔT, °C
228.6	2.07	8760	15.4
229.6	1.91	3410	14.4
230.6	1.95	1030	13.4
231.1	1.84	707	12.9
231.6	1.88	289	12.4
232.6	2.02	60.8	11.4
233.6	1.91	17.0	10.4
234.6	1.92	2.97	9.4

$n_{av} = 1.93 \pm 0.07$

narrow temperature range, suggesting that $\sigma\sigma_e \gg \sigma\Delta\sigma$, and eq 8 then reduces to

$$\text{slope} = -8b_0\sigma\sigma_e T_m^{\,0}/k_b\Delta H \qquad (9)$$

Here, for PBFP, $\Delta H = 6.41$ J/cm^3, $b_0 = 1.18$ nm, and $z = 2$, since the results from the Avrami analysis indicate the growth is two-dimensional. If the average value of the slope is determined (−85 500 K^2), the product of the surface free energies, $\sigma\sigma_e$, is 1.6 ergs^2/cm^4. The product of the surface energies[24,25] from linear growth rate experiments for many common homopolymers (polyethylene ~1280, i-polystyrene ~266, and poly(chlorotrifluorethylene) ~200 ergs^2/cm^4) are at least 2 orders of magnitude greater than the value determined here for PBFP.

(b) 2-D to 3-D Region. Figure 12 shows the extent of transformation versus log time for the two-dimensional hexagonal mesophase to the three-dimensionally ordered crystalline orthorhombic phase of PBFP as obtained via the DSC method. Both the base-line subtraction and short time extent of conversion recovery techniques were utilized to obtain these plots from the rate of energy evolution curves. Figure 13 shows Avrami plots of this data. By least-squares fit of the data in the initial linear portion of each curve, an average value of $n = 1.91 \pm 0.08$ was obtained. Values of k were determined by utilizing an n of 2.0 and a fractional transformation of 0.2 and are shown in Table V. Unlike the isotropic

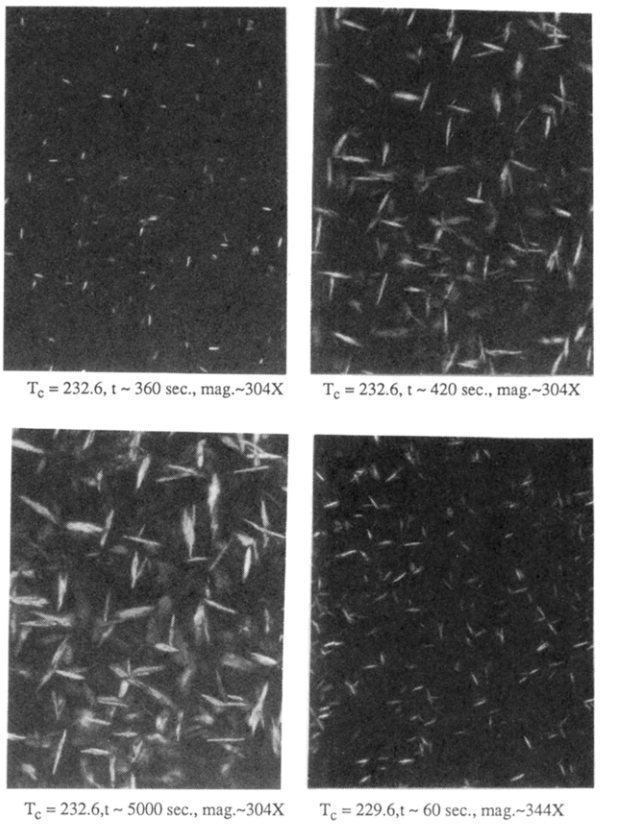

Figure 9. Photomicrographs of the isotropic melt to 2-D mesophase transformation in PBFP for the given conditions.

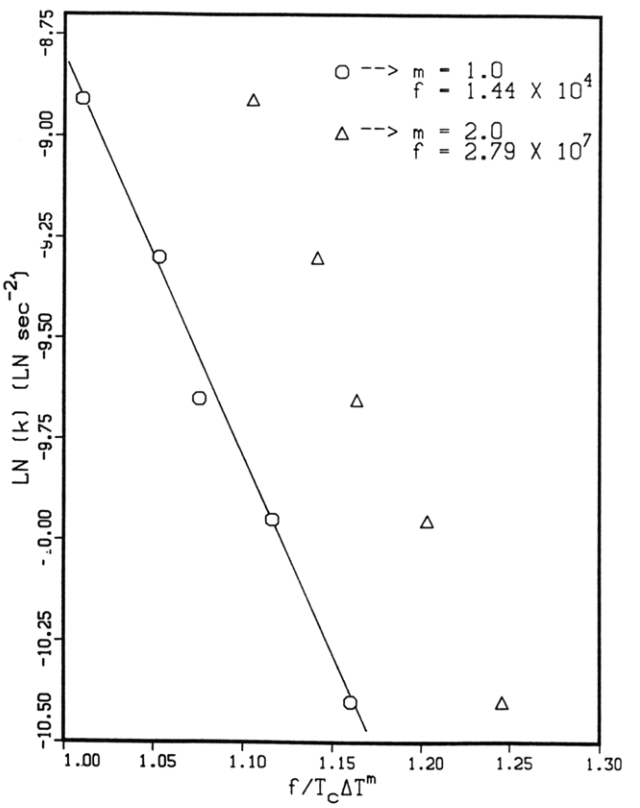

Figure 10. Plots of ln k versus $1/T_c\Delta T$ and $1/T_c\Delta T^2$ for the isotropic melt to 2-D mesophase transformation of PBFP (DSC method).

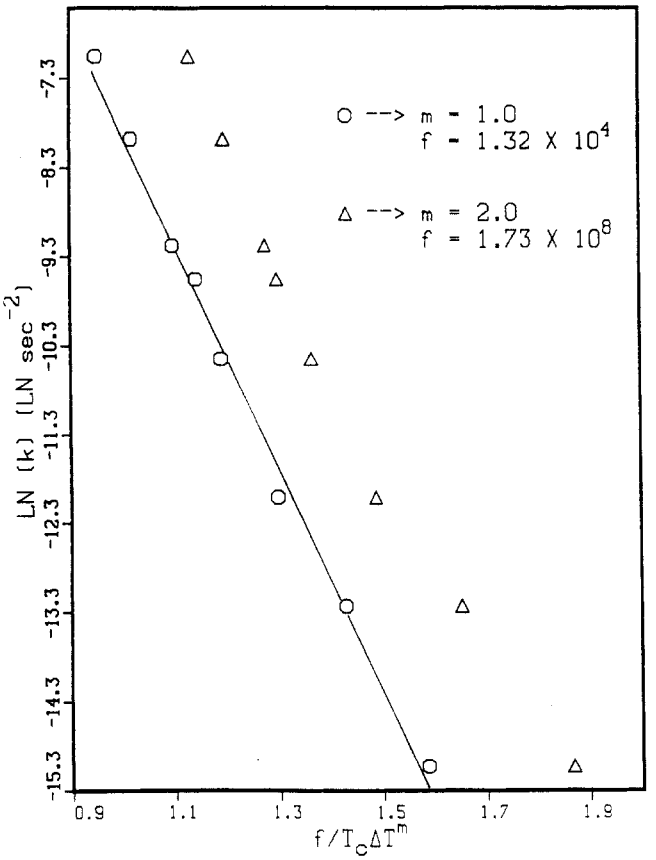

Figure 11. Plots of ln k versus $1/T_c\Delta T$ and $1/T_c\Delta T^2$ for the isotropic melt to 2-D mesophase transformation of PBFP (DLI method).

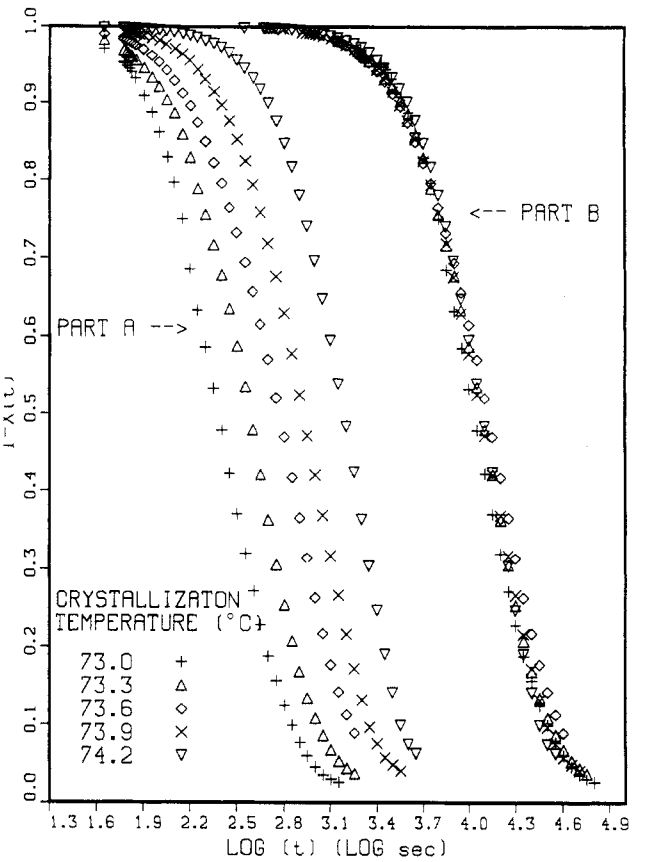

Figure 12. The extent of transformation versus log time curves for PBFP at several crystallization temperatures for the 2-D mesophase to 3-D crystalline transformation via the DSC method. Part A: the actual curves. Part B: the actual curves shifted along the log t axis (ie: superimposed).

melt to 2-D transformation in PBFP, this transformation displayed a small birefringence change and therefore was not readily amenable to measurement by the DLI method.

Plots of ln k versus $1/T_c\Delta T$ and $1/T_c\Delta T^2$, where $\Delta T = T(1) - T_c$, made for this transformation are shown in Figure 14. The low supercooling portion of the plot versus $1/T_c\Delta T$ yielded a slope of −67 400 K^2. The large, negative change in the rate constants over this small crystallization range, in addition to the small undercooling needed for crystallization, indicates the nucleation was heterogeneous. In accord with an Avrami nucleation parameter of 2, it is concluded that the growth is two-dimensional.

Two important points may be made about this transition. First, at comparable undercoolings from their respective transition temperatures, the 2-D to 3-D transformation takes place at a rate that is an order of magnitude faster than in the isotropic to 2-D transformation. *Second, over the measurable crystallization range (1.2 °C), the rate constant k changes by 2 orders of magnitude.* For extrapolation to a temperature range of 6 °C (DLI measurement range for the isotropic to 2-D transformation), a change in k of over 5 orders of magnitude is expected. From this fact it is concluded that this transformation is more temperature sensitive than the isotropic to 2-D transformation and also that the crystallization transformation is nucleation-controlled. From the slope of the low supercooling end of the plot of ln k versus $1/T_c\Delta T$, the value of the product of the surface free energies, $\sigma\sigma_e$, was determined to be 30 ergs^2/cm^4 for ΔH = 88.2 J/cm^3, b_0 = 0.94 nm, and again z = 2. Although this $\sigma\sigma_e$ is larger than the value obtained for the isotropic to mesophase transformation, it is still at least an order of magnitude smaller than that found for normal homopolymers of comparable enthalpy of transformation.

Comparison of the DLI and DSC Methods. From the isotropic melt to 2-D mesophase measurements on PBFP, the DSC and DLI techniques were compared in evaluating the Avrami parameters. Figure 15 shows the DSC Avrami plots on the same scale as the DLI data of Figure 8. The curves show low conversion superposability with the DLI data but do not show the long time slowing down of crystallization rate apparent in the DLI data. The inadequacy of the DSC for measuring this slow, long time transformation may be readily attributable to the fact that the DSC yields the derivative of the transformation (as opposed to the DLI method which yields the actual transformation curve). This being the case, the rate of energy evolution at long times is too small to be detected accurately by the DSC, and therefore it does not appear in the Avrami plots. This is a particularly acute problem in the isotropic to mesophase transformation in thermotropic mesophase forming materials due to the extremely small enthalpy of transition especially when compared to normal homopolymers. In contrast the DLI method measures the cumulative effect of the crystallization transformation and is much more suitable for measuring slower rates so long as there is a significant birefringence change under quiescent conditions.

Since the DSC is inadequate for measuring the long time, slow transformation in PBFP, it is necessary to consider the effect of this error on the values of $X(t)$, in which the denominator depends on the total heat of fusion of the sample. This is most easily accomplished by examining the Avrami plots of the DSC data after including

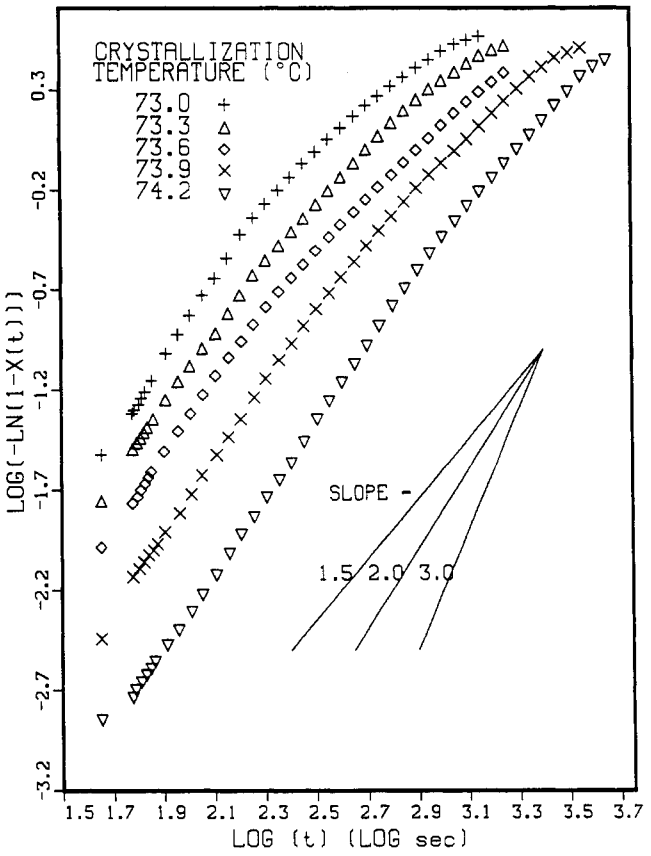

Figure 13. DSC Avrami plots for the 2-D mesophase to 3-D crystalline transformation in PBFP.

Table V
Avrami Parameters for the 2-D Mesophase to 3-D Ordered Crystalline Transformation in PBFP

T_c, °C	n	10^7k, $s^{-2.0}$	ΔT, °C
73.0	2.01	40600	15.6
73.3	1.81	18000	15.3
73.6	1.84	6270	15.0
73.9	1.95	2210	14.7
74.2	1.91	927	14.4

$n_{av} = 1.90 \pm 0.08$

an additional (yet arbitrary) 50% increase in the ΔH_∞ value for $X(t)$. The result is shown in Figure 16 for two different crystallization temperatures, where increasing ΔH_∞ produces several interesting effects. First, it demonstrates that indeed the DSC is insensitive to the long time crystallization effects (small enthalpy changes over long times) that are observable in the DLI Avrami plots. Further evidence for this fact is that the measured ΔH_∞ upon isothermal crystallization is usually substantially less than that found on subsequent reheating of the specimen. We have found errors as high as 40% between the two measurements for samples that crystallize slowly over long times (as is the case for the sample crystallized at 231.5 °C). Second and most importantly, the values of n are unchanged from the previous results (i.e., the slope of the initial portion of the curves remains unchanged), and third, the plots are shifted by a relatively constant log time factor to longer times. This produces a nonlinear effect on the actual values of the rate constants and shifts them to lower values. However values for ln k are moved to lower values by a relatively constant factor. This does not affect the slopes of the plots of ln k versus $1/T_c\Delta T_m$ and does not affect values obtained for the energies and sizes of the nuclei. In essence only small errors in n or in the plots of ln k versus $1/$

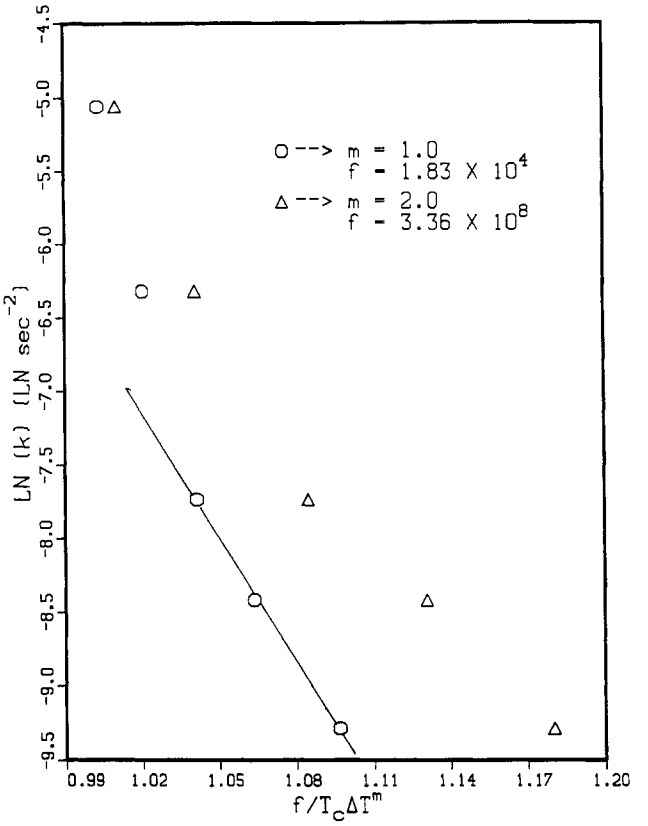

Figure 14. Plots of ln k versus $1/T_c\Delta T$ and $1/T_c\Delta T^2$ for the 2-D mesophase to 3-D crystalline transformation in PBFP.

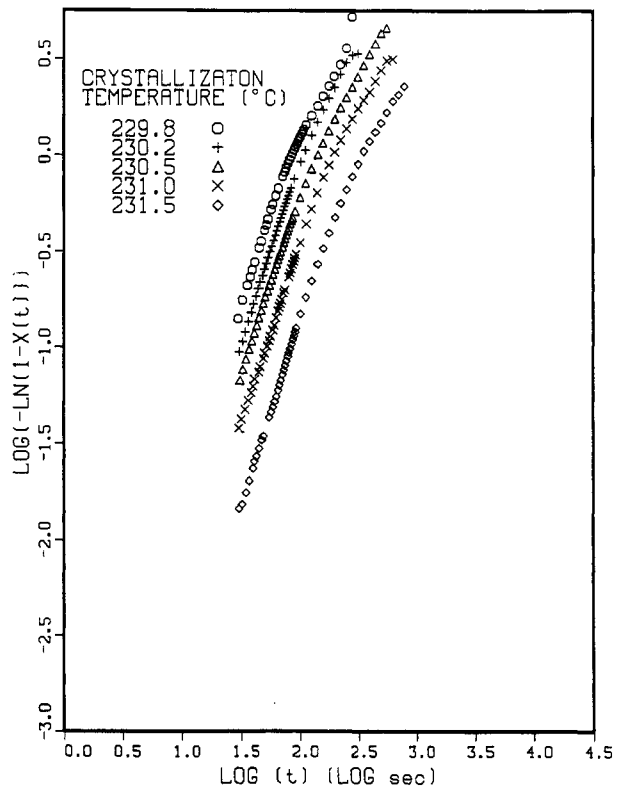

Figure 15. Avrami plots of the isotropic melt to 2-D mesophase transformation of PBFP for the DSC method shown at the scale of the Avrami plots of the DLI data of Figure 8.

$T_c\Delta T$ are introduced because of the inadequacy of the DSC method for measuring slow changes in sample crystallinity (enthalpy) over long times.

Another crucial problem with the DSC is its limited capacity for measuring the rate of energy evolution (and thereby the extent of transformation) in at least the first

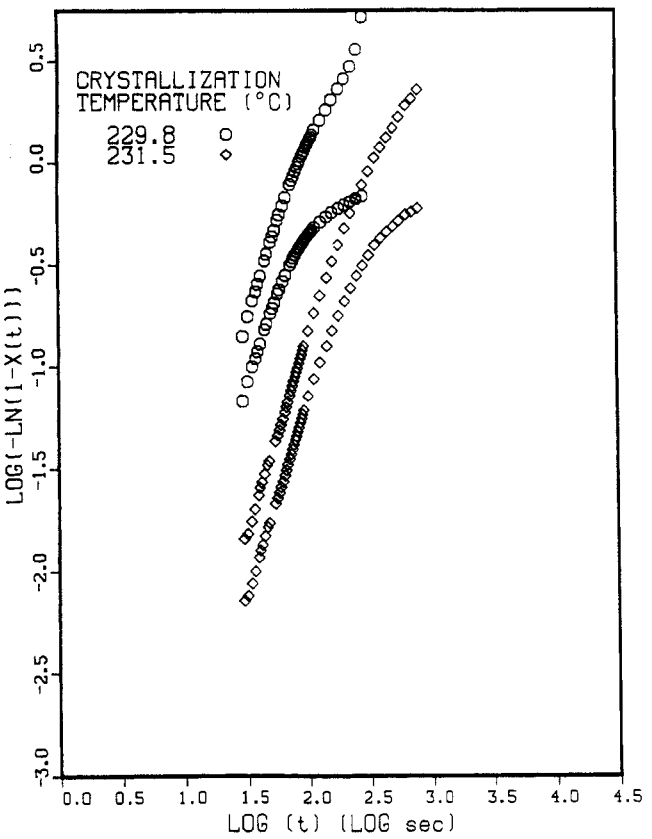

Figure 16. Avrami plots of the DSC data for the isotropic melt to 2-D transformation of PBFP after arbitrarily incraeasing the total heat of fusion by 50% (the bottom curve of each set).

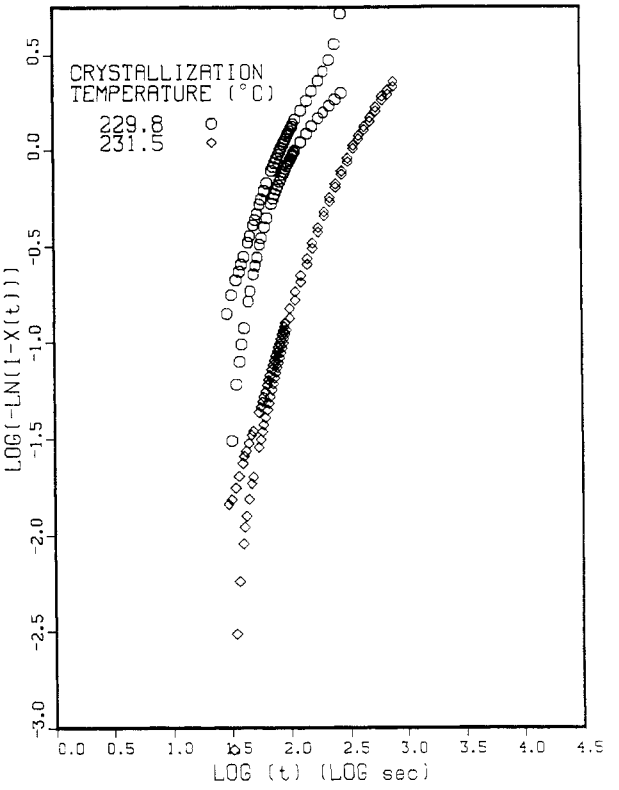

Figure 17. Avrami plots of the DSC data for the isotropic melt to 2-D transformation of PBFP at two crystallization temperatures displaying the error encountered whenever the initial extent of transformation is neglected. The bottom curve in each set shows the unrecovered plots.

30 s of crystallization, even after base-line subtraction is performed. As such it was necessary to recover the extent of transformation associated with the initial 30 s of crystallization using the recrystallization/reheating technique outlined above. Figure 17 shows the result whenever the initial heat of crystallization is omitted or neglected when generating Avrami plots. Excessive curvature in the plots occurs at short times, thereby making the evaluation of the Avrami parameters impossible. Even for the curves at 231.5 °C, where only a small portion of the crystallization (~1.4%) takes place in the first 30 s of the transformation, significant curvature is noted in the uncorrected curve and this would introduce significant errors into the evaluation of n and k. By comparison, neither long time, slow conversion nor short time, fast conversion corrections are necessary for the DLI measurements, and these advantages make it the preferred technique as long as the change in sample birefringence is sufficiently large and representative of the phase transformation.

Conclusions

The mechanisms for the nucleation and growth of PBFP have been established for (1) the isotropic to 2-D thermotropic mesophase and for (2) the 2-D thermotropic mesophase to 3-D crystal transformations. The product of the surface free energies, $\sigma\sigma_e$, for both transformations have been estimated to be at least an order of magnitude less than the values usually observed for the isotropic to crystalline transformation in normal homopolymers. This situation implies that the interfaces, associated with the transformation in points (1) and (2) above, are mildly compatible because of their mesophase nature. Sidechain mobilities from MAS NMR[25] support this picture. The small undercoolings necessary to crystallize these samples and the extremely large sensitivity of the rate parameter on undercooling indicate that relatively small forces must be overcome for the crystallization of these polymers in both transformation regions.

A comparison of the DLI and DSC techniques for measuring the extent of transformation in crystallizing systems has also been made. The DSC technique suffers from two major drawbacks, namely, *insensitivity to small changes in the enthalpy of the material under study due to slow, long time crystallization and problems associated with fluctuations in the rate of energy evolution signal encountered during mode switching operations.* Difficulties encountered in measuring crystallization transformations using the DSC technique have been mitigated by procedures introduced in this work, namely, (i) a base-line subtraction technique and (ii) a recrystallization/reheating technique. This paper shows that the initial portion of crystallization may be recovered satisfactorily. In general these techniques should have wide application for kinetic measurements using the DSC. However, overall, the DLI technique suffers from neither of the problems associated with the DSC technique and is the preferred technique if the birefringence change during crystallization is adequate for measurement.

Acknowledgment. Thanks are due to the National Science Foundation (Polymer Program, Grant DMR 8509412) and the Office of Naval Research (Chemistry Program, Grant N0001485K0358) for research support. We also wish to thank Dr. T. Nishikawa of the Nippon Soda Co. for supplying the polymerization grade trimer used for the synthesis of these polyphosphazenes and Dr. F.-T. Lin, Chemistry Department, University of Pittsburgh, for the solution NMR analysis.

References and Notes

(1) Singler, R. E.; Hagnauer, G. L. *Polyphosphazenes: Structure and Applications*; Academic Press: New York, 1978.
(2) Allcock, H. R.; Fuller, T. J.; Matsumura, K.; Austin, P. E. *Polym. Prepr. (Am. Chem. Soc., Div. Polym. Chem.* **1983**, *21*, 111.
(3) Kojima, M.; Magill, J. H. *Polymer* **1985**, *26*, 1971.
(4) Alexander, M. N.; Desper, C. R. *Macromolecules* **1977**, *10*, 721.
(5) Sun, D. C.; Magill, J. H. *Polym. Pap.* **1987**, *28*, 1243.
(6) Kojima, M.; Magill, J. H. *Polymer* **1989**, *30*, 579.
(7) Price, F. P.; Wendorf, J. H. *J. Phys. Chem.* **1971**, *75*, 2839.
(8) Price, F. P.; Wendorf, J. H. *J. Phys. Chem.* **1971**, *75*, 2849.
(9) Price, F. P.; Wendorf, J. H. *J. Phys. Chem.* **1972**, *76*, 276.
(10) Price, F. P.; Fritzsche, J. *J. Phys. Chem.* **1973**, *77*, 386.
(11) Jabarin, S. A.; Stein, R. S. *J. Phys. Chem.* **1973**, *77*, 399.
(12) Jabarin, S. A.; Stein, R. S. *J. Phys. Chem.* **1973**, *77*, 409.
(13) Adamski, P.; Czyzewski, R. *Sov. Phys. Crystallogr.* **1978**, *23*, 82.
(14) Adamski, P.; Czyzewski, R. *Sov. Phys. Crystallogr.* **1977**, *22*, 725.
(15) Warner, S. B.; Jaffe, M. *J. Cryst. Growth* **1980**, *48*, 184.
(16) Grebowicz, J.; Cheng, S. Z. D.; Wunderlich, B. *J. Polym. Sci., Polym. Phys. Ed.* **1986**, *24*, 675.
(17) Liu, X.; Hu, S.; Xu, M.; Zhou, Q.; Duan, X. *Polymer* **1989**, *30*, 273.
(18) Masuko, T.; Okuizumi, K.; Yonetake, K.; Magill, J. H. *Macromolecules* **1989**, *22*, 4636.
(19) Mujumdar, A.; Young, S. G.; Merker, R. L.; Magill, J. H. *Makromol. Chem.* **1990**, *190*, 2293.
(20) Magill, J. H. *Nature* **1960**, *187*, 770–771.
(21) Turnbull, D.; Fisher, J. C. *J. Chem. Phys.* **1949**, *17*, 71–74.
(22) Wunderlich, B. *Macromolecular Physics*; Academic Press: New York, 1976; Vol. 2.
(23) Magill, J. H. In *Treatise on Materials Science and Technology*; Academic Press: New York, 1977; Vol. 10A.
(24) Hoffman, J. D.; Davis, G. T.; Lauritzen, J. I., Jr. *Treatise on Solid State Chemistry*; Plenum Press: New York, 1972.
(25) Young, S. G.; Magill, J. H. *Macromolecules* **1989**, *22*, 2549.

Registry No. PBFP, 28212-50-2.

A Study of the Isothermal Crystallization Kinetics of Polyphosphazene Polymers. 3. Poly[bis(phenylphenoxy)phosphazene]

Richard J. Ciora, Jr., and Joseph H. Magill*

Material Science and Engineering Department, University of Pittsburgh, Pittsburgh, Pennsylvania 15261.

Received July 24, 1989; Revised Manuscript Received November 7, 1989

ABSTRACT: In this study the isothermal crystallization kinetics of poly[bis(phenylphenoxy)phosphazene] have been examined utilizing (i) a modified differenital scanning calorimeter (DSC) technique and (ii) a depolarized light intensity (DLI) technique. The kinetics of transformation of the isotropic to 2-D pseudohexagonal mesophase (ie. the sub T_m transformation) as well as the mesophase to 3-D orthorhombic phase (i.e. the sub $T(1)$ transformation) have been measured and analyzed by using Avrami analysis. Classical nucleation theory has been applied for estimating the surface free energy values for nucleation/crystallization behavior corresponding to the phase transformations in the sub $T(1)$ and sub T_m regions. These results have been compared with poly[bis(trifluoroethoxy)phosphazene]. It has been found that the polymers display similar transformation kinetics. Both show very high, negative growth rates versus inverse undercooling coefficients as well as inordinately small surface free energy products compared to normal homopolymers, in accord with the compatibility of the mesophase transformation interfaces.

Introduction

Since the 1960s many stable linear high molecular weight polyphosphazene polymers have been synthesized, and some of their physical and thermal properties have been characterized. The basic structure of these polymers consists of an alternating phosphorous and nitrogen backbone as shown in Figure 1. Because of the variety of substituent groups that may be attached to the phosphorous atom, an extensive array of polymers with diverse properties can be produced.[1,2]

Many of the semicrystalline polyphosphazenes exhibit three thermal transitions on heating; a glass transition at T_g, a mesomorphic transition at $T(1)$ from the three dimensionally ordered orthorhombic (γ-form) crystalline state to the two dimensionally ordered pseudo-hexagonal (δ-form) state followed by isotropization at T_m. Recently, considerable interest has focused on determing the structure of these polymers in both the crystalline and mesomorphic states as it relates to the sample's thermal history.[3,4] Although considerable effort has gone into elucidating the structure of these materials in the various phases, few investigations into molecular aspects of the mechanisms and energetics that control the formation of these phases in polyphosphazenes have been conducted.[5-7] A basic understanding of the energetics and mechanisms of the formation of the different phases and their dependence on thermal history is necessary from a physical properties perspective because such properties as toughness, elasticity, permeability, etc. can be significantly altered by polymeric microstructure. It is through isothermal bulk crystallization studies that such information may be obtained.

In this paper the kinetics of the isothermal crystallization of the polyphosphazene polymer poly[bis(phenylphenoxy)phosphazene] or PB(4-Ph)PP (shown in Figure 1) are investigated by using the depolarized light intensity[8] (DLI) technique. In part I[9] of this series the DLI technique had been examined as a general technique for studying phase transformations in polyphosphazene polymers. In part II kinetic measurements[5] for the crystallization transformation in poly[bis(trifluoro-

0024-9297/90/2223-2359$02.50/0